Correlation of *BRAF*^{V600E} Mutation and Glucose Metabolism in Thyroid Cancer Patients: An ^{18}F-FDG PET Study

James Nagarajah[1,2], Alan L. Ho[3], R. Michael Tuttle[2], Wolfgang A. Weber[1], and Ravinder K. Grewal[1]

[1]*Molecular Imaging and Therapy Service, Memorial Sloan Kettering Cancer Center and Weill Cornell Medical College, New York, New York;* [2]*Endocrinology Service, Memorial Sloan Kettering Cancer Center and Weill Cornell Medical College, New York, New York; and* [3]*Head and Neck Oncology Service, Memorial Sloan Kettering Cancer Center and Weill Cornell Medical College, New York, New York*

There is significant interest in a better understanding of the genetic underpinnings of the increased glucose metabolic rates of cancer cells. Thyroid cancer demonstrates a broad variability of ^{18}F-FDG uptake as well as several well-characterized oncogenic mutations. In this study, we evaluated the differences in glucose metabolism of the *BRAF*^{V600E} mutation versus *BRAF* wild-type (*BRAF*-WT) in patients with metastatic differentiated thyroid cancer (DTC) and poorly differentiated thyroid cancer (PDTC). **Methods:** Forty-eight DTC and 34 PDTC patients who underwent ^{18}F-FDG PET/CT for tumor staging were identified from a database search. All patients were tested for the *BRAF*^{V600E} mutation and assigned to 1 of 2 groups: *BRAF*^{V600E} mutated and *BRAF*-WT. ^{18}F-FDG uptake of tumor tissue was quantified by maximum standardized uptake value (SUV_{max}) of the hottest malignant lesion in 6 prespecified body regions (thyroid bed, lymph nodes, lung, bone, soft tissue, and other). When there were multiple lesions in 1 of the prespecified body regions, only the 1 with the highest ^{18}F-FDG uptake was analyzed. **Results:** In the DTC cohort, 24 tumors harbored a *BRAF*^{V600E} mutation, whereas 24 tumors were *BRAF*-WT. ^{18}F-FDG uptake of *BRAF*^{V600E}-positive lesions (median SUV_{max}, 6.3; $n = 53$) was significantly higher than that of *BRAF*-WT lesions ($n = 39$; median SUV_{max}, 4.7; $P = 0.019$). In the PDTC group, only 5 tumors were *BRAF*^{V600E}-positive, and their ^{18}F-FDG uptake was not significantly different from the *BRAF*-WT tumors. There was also no significant difference between the SUV_{max} of all DTCs and PDTCs, regardless of *BRAF* mutational status ($P = 0.90$). **Conclusion:** These data suggest that *BRAF*^{V600E}-mutated DTCs are significantly more ^{18}F-FDG–avid than *BRAF*-WT tumors. The effect of *BRAF*^{V600E} on tumor glucose metabolism in PDTC needs further study in larger groups of patients.

Key Words: thyroid cancer; *BRAF*^{V600E}-mutation; ^{18}F-FDG uptake; DTC; PDTC

J Nucl Med 2015; 56:662–667
DOI: 10.2967/jnumed.114.150607

Thyroid cancer is a genetically heterogeneous disease that demonstrates a broad spectrum of glucose metabolic rates as shown by ^{18}F-FDG PET/CT studies (*1–3*). Several studies have demonstrated that tumor ^{18}F-FDG uptake of poorly differentiated thyroid cancer (PDTC) is higher than that of differentiated thyroid cancer (DTC). Furthermore, survival of patients with thyroid cancer has been shown to be inversely correlated to the intensity of ^{18}F-FDG uptake as measured by maximum standardized uptake values (SUV_{max}) (*4*). These data suggest that ^{18}F-FDG uptake is a reflection of tumor proliferation and aggressiveness. However, some well-differentiated thyroid cancers and even benign thyroid nodules can exhibit high ^{18}F-FDG uptake (*5*). These clinical observations suggest that ^{18}F-FDG uptake by thyroid tumors is not necessarily caused by rapid proliferation but may be due to genetic alterations causing accelerated glucose metabolism.

About 45% of papillary DTCs harbor a *BRAF*^{V600E} mutation, whereas *RAS* mutations and *RET/PTC* rearrangements are less common (*6,7*). On the other hand, *RAS* mutations are more frequent in PDTCs (*8,9*). DTCs harboring a *BRAF*^{V600E} mutation show a higher expression of glucose transporter 1 than those with wild-type (WT) *BRAF,* indicating that tumors with *BRAF*^{V600E} may show a higher ^{18}F-FDG uptake (*10*). A recently published multicenter study indicated a poorer prognosis for DTC patients harboring *BRAF*^{V600E} mutation (*11*). Previous studies have also indicated that high ^{18}F-FDG uptake in thyroid cancer points to poorer prognosis (*4*). However, to our knowledge, no published clinical data suggest a direct association between *BRAF*^{V600E} status and ^{18}F-FDG uptake.

In colorectal cancer as well as melanoma, *BRAF*^{V600E} has been shown to regulate glycolysis independently of cell-cycle progression or cell death, also suggesting that *BRAF*^{V600E} mutations may be associated with increased glycolysis (*12,13*).

We therefore hypothesized that thyroid cancers with *BRAF*^{V600E} mutations demonstrate higher ^{18}F-FDG uptake than *BRAF*-WT, irrespective of histologic characteristics. We tested this hypothesis in a retrospective study of DTC and PDTC patients who underwent ^{18}F-FDG PET/CT for tumor staging and for whom the *BRAF*^{V600E} mutational status was known.

MATERIALS AND METHODS

Patients

We performed an automated search for all DTC and PDTC patients who underwent ^{18}F-FDG PET/CT and had a *BRAF* mutational status analysis performed on their primary tumors. Patients with secondary malignancies were excluded. The classification of tumors as DTC or PDTC is based on the interpretation of the histologic sections of the primary tumor by our institution's Department of Pathology.

Sequenom mass spectrometry or next-generation sequencing was used to assess the mutational status of all patients. Not all of the tumor samples were investigated for other mutations such as *RAS* or *RET/PTC*;

Received Oct. 28, 2014; revision accepted Feb. 25, 2015.
For correspondence or reprints contact: James Nagarajah, Molecular Imaging and Therapy Service, Memorial Sloan Kettering Cancer Center, 1275 York Ave., New York, NY 10065.
E-mail: nagarajj@mskcc.org
Published online Mar. 26, 2015.

therefore, the patients were classified as *BRAF*^{V600E} or *BRAF*-WT. Patient characteristics are provided in Table 1.

Our institutional review board approved this retrospective study, and the requirement to obtain informed consent was waived.

^{18}F-FDG PET/CT Imaging

Because we accrued patients over a period of 14 y, the PET/CT scans had been obtained with multiple scanner types. However, patient preparation and image acquisition protocols were comparable over the years. All scans were acquired using PET/CT cameras, including Discovery LS, Discovery ST, and Discovery STE (all GE Healthcare) or Biograph LSO-16 (Siemens Medical Solutions). No information on the scanner system was available for 22% of the patients. Patients were instructed to fast for at least 6 h before ^{18}F-FDG administration, and blood glucose levels were required to be less than 200 mg/dL at the time of injection. The scans were acquired from the upper thighs to the base of the skull (5–7 bed positions) 60–90 min after injection of about 400 MBq of ^{18}F-FDG. CT was performed for attenuation correction and anatomic localization. Immediately after the CT image acquisition, PET data were acquired for 3–5 min per bed position. The attenuation-corrected PET data were reconstructed using an ordered-subset expectation maximization iterative reconstruction.

Image Analysis

Lesions with the typical appearance of local recurrence or metastases on PET or CT were analyzed. Criteria for metastatic disease were focal ^{18}F-FDG uptake above regional background that was not explained by the physiologic pattern of ^{18}F-FDG uptake and excretion. In the absence of focal ^{18}F-FDG uptake, standard CT morphologic criteria were used to define a malignant lesion. These included lytic bone lesions and lung nodules larger than 1 cm in diameter. The location of the lesions was classified as thyroid bed, lymph node, lung, bone, soft tissue, or other (Table 2). For each of these sites, ^{18}F-FDG uptake was quantified for the lesion with the highest ^{18}F-FDG uptake using SUVs normalized to the body weight of the patient. For measurement of SUVs, a spheric volume of interest encompassing the complete lesions was defined using the AW Volume Viewer Software (GE Healthcare). Areas of physiologic ^{18}F-FDG uptake such as the myocardium were carefully excluded. Lesion size was measured on CT if the lesion was well delineated on the CT images. For lesions with insufficient contrast on CT (mostly bone lesions), tumor size was measured on PET as the maximum diameter of an isocontour defined by 45% of the maximum uptake within the lesion.

The highest standardized uptake value (SUV) (SUV_{max}) within the volume of interest was recorded. Only 1 lesion in the predefined sites (Table 2) was analyzed. For lesions considered malignant on CT, but showing no focal ^{18}F-FDG uptake on PET, an SUV_{max} of -1 was recorded. We used this approach instead of recording the actual SUV at the site of the lesion because physiologic differences in background activity would otherwise significantly affect the SUV measurements. For example, a liver lesion that shows no focal ^{18}F-FDG uptake could be assigned a higher SUV than a lung lesion with focal ^{18}F-FDG uptake. Therefore, it seemed more appropriate to use a single SUV for all lesions that were not seen with positive contrast on PET.

We also analyzed whether there were differences between the SUVs of *BRAF*^{V600E} and *BRAF*-WT patients when only the single lesion with the highest ^{18}F-FDG uptake was analyzed. Because of the small number of patients with PDTC, this analysis was not performed for this group of patients.

Some of the ^{18}F-FDG–positive lesions were small enough to be affected by partial-volume effects. In an attempt to minimize this effect on the comparison of the analyzed 2 groups, we performed a statistical test to rule out any differences in the distribution of the sizes of the lesions in the *BRAF*^{V600E} and *BRAF*-WT groups (P = 0.27, Mann–Whitney U test).

Statistical Analysis

The statistical software GraphPad Prism (version 6.0; GraphPad Software, Inc.) was used to analyze the data. All reported P values were calculated using the 2-sided Mann–Whitney U test or Fisher exact test, and a P value of less than 0.05 was considered significant.

RESULTS

Patient Characteristics

Forty-eight DTCs and 34 PDTCs were identified from the database search (2001–2005, n = 1; 2006–2010, n = 44; 2011–2013, n = 37). All patients had undergone surgery before the PET/CT study, and all but 2 patients with PDTC had received radioiodine therapy. Radioiodine scans under thyroid-stimulating hormone (TSH) stimulation were negative in all patients, but there was evidence for disease progression based on thyroglobulin levels or abnormal morphologic imaging findings. Seven DTC patients died during follow-up (n = 5 [21%] *BRAF*^{V600E} and 2 [8%] *BRAF*-WT). Of the PDTC patients, 12 died during follow-up (n = 2 [40%] *BRAF*^{V600E} and 10 [34%] *BRAF*-WT).

In the DTC group, 24 tumors had a confirmed *BRAF*^{V600E} mutation, and 24 were classified as *BRAF*-WT^{V600E} (10 of those designated *BRAF*-WT had a *RAS* mutation, and the other mutational status was unknown). The PDTC group comprised 34 patients; 5 had a *BRAF*^{V600E} mutation and 29 were classified as *BRAF*-WT (15 of these had a *RAS* mutation). Patient characteristics including sex, age, TNM status, thyroglobulin/TSH values, and radioiodine treatments are given in Table 1. *BRAF*^{V600E} and *BRAF*-WT groups did not differ with respect to the time from pathologically confirmed diagnosis to PET (P = 0.86 for DTC and 0.16 for PDTC patients, Mann–Whitney U test). We also performed a statistical test to verify a homogeneous distribution of the age of patients in the compared groups (DTC group with *BRAF*^{V600E} and *BRAF*-WT, P = 0.24; PDTC group with *BRAF*^{V600E} and *BRAF*-WT, P = 0.10, Mann–Whitney U test).

^{18}F-FDG PET

In the DTC patients, 101 lesions were analyzed. The number of ^{18}F-FDG–positive lesions in the *BRAF*^{V600E} and *BRAF*-WT groups was 54 (53%) and 39 (39%), respectively. The number of ^{18}F-FDG–negative lesions was 3 (3%) in the *BRAF*^{V600E} group and 5 (5%) in the *BRAF*-WT group. Twenty of the 39 (51%) ^{18}F-FDG–positive lesions in the *BRAF*-WT lesions harbored *RAS* mutations.

In the group of PDTCs, 60 lesions were analyzed. The number of ^{18}F-FDG–positive lesions in the *BRAF*^{V600E} group was 12 (20%), whereas none of the lesions in this group was ^{18}F-FDG–negative. There were 37 (62%) ^{18}F-FDG–positive and 11 (18%) ^{18}F-FDG–negative lesions in the *BRAF*-WT PDTC group. Twelve of these 48 (25%) lesions in the *BRAF*-WT group harbored *RAS* mutations. Details about lesion characteristics are shown in Tables 1 and 2.

In the DTC group of patients, the *BRAF*^{V600E}-positive lesions showed a significantly higher SUV_{max} than *BRAF*-WT lesions (P = 0.019, Mann–Whitney U test) (Table 3; Fig. 1). There was also a significant difference when comparing only the single lesion with the highest SUV_{max} per patient in the *BRAF*^{V600E} and *BRAF*-WT groups (P = 0.04, Mann–Whitney U test).

In contrast, there was no significant difference of ^{18}F-FDG uptake in the PDTC group between *BRAF*^{V600E} and *BRAF*-WT (P = 0.85, Mann–Whitney U test, Fig. 2). Neither did we observe a difference of SUV_{max} when comparing all DTC with PDTC lesions, regardless of mutational status (P = 0.90, Mann–Whitney U test, Table 3, Fig. 3). SUV_{max} was approximately twice as high in *BRAF*-WT PDTC when compared with *BRAF*-WT DTC (P = 0.11, Mann–Whitney U test). Patients' images are given in Figure 4.

TABLE 1
Patient Characteristics of *BRAF*^{V600E} and *BRAF*-WT Groups

Characteristic	DTC		PDTC	
	BRAF^{V600E}	*BRAF*-WT	*BRAF*^{V600E}	*BRAF*-WT
n				
PT genotype	24 (2)*	24 (2)*	5	29
Lesions†	57	44	12	48
Lesions per patient				
<5	13	16	3	17
5–10	1	2	0	6
>10	10	7	2	6
^{18}F-FDG PET				
Positive	21	19	5	20
Negative	3	5	0	9
Age (y)				
Mean ± SD	68 ± 11‡	64 ± 11‡	72 ± 11§	61 ± 13§
Sex				
Female	13	15	1	16
Male	11	9	4	13
TNM				
TX	4	3	1	0
T1/a/b	1/1/2	4/0/0	0/0/0	0/0/2
T2/a/b	2/0/0	5/0/0	1/0/0	7/0/0
T3/a/b	8/0/0	5/0/0	1/0/0	10/4/1
T4/a/b	2/3/1	3/1/3	0/2/0	0/2/3
NX/0	4/6	4/11	1/1	0/18
N1/a/b	6/3/5	3/3/3	1/0/2	3/4/4
MX/0/1	4/19/1	4/14/6	1/2/2	0/23/6
Radioiodine (GBq)‖				
Median/minimum/maximum	5.8/3.7/30.5	7.4/2.6/32.7	2.7/1.1/4.4	7.4/1.9/24.5
TSH (mU/L)¶				
Median/minimum/maximum	0.07/0.01/4.92	0.03/0.02/1.63	0.1/0.02/1.7	0.04/0.02/15.2
Thyroglobulin (ng/mL)#				
Median/minimum/maximum	6.9/0.2/1,930	360/0.3/37,000	46.9/2.2/670	270/1.7/1,4400
PET to D				
Mean ± SD	31 ± 41**	24 ± 36**	40 ± 51††	11 ± 26††

*No. of patients, with follicular variant of PTC in parentheses.
†Only 1 lesion per site per patient (Table 2) was analyzed.
‡$P = 0.24$, Mann–Whitney *U* test.
§$P = 0.10$, Mann–Whitney *U* test.
‖All patients with DTC received radioiodine; amount of ^{131}I missing in $n = 26$, $n = 2$ patients with PDTC did not receive radioiodine, $n = 1$ no data about radioiodine available, $n = 8$ amount of ^{131}I missing.
¶For $n = 2$ patients with PDTC, no data were available.
#For $n = 4$ patients with DTC and $n = 3$ patients with PDTC, no thyroglobulin data were available and $n = 4$ patients with DTC had thyroglobulin level below 0.3 ng/mL, but for all of these patients, progress was stated with CT. Difference of thyroglobulin values in WT DTC was significantly higher than in *BRAF*^{V600E} group ($P = 0.009$).
**$P = 0.59$, Mann–Whitney *U* test.
††$P = 0.16$, Mann–Whitney *U* test.
PET to D = time difference between PET and diagnosis verified by molecular pathology, given in months.

TABLE 2
Localization of Lesions for *BRAF*^{V600E} and *BRAF*-WT Groups

Site	DTC		PDTC	
	BRAF^{V600E}	*BRAF*-WT	*BRAF*^{V600E}	*BRAF*-WT
Thyroid bed	11*	2*	4	6
Lymph node	20†	12†	3	13
Lung	17 (3)‡	19 (5)‡	4	9 (9)
Bone	3	10	0	4 (2)
Soft tissue	3	0	1	3
Other	3	1	0	2
Total number	57	44	12	48

*$P = 0.008$, Fisher exact test.
†$P = 0.031$, Fisher exact test.
‡$P = 0.049$, Fisher exact test.
Data in parentheses are no. of ^{18}F-FDG–negative lesions. Other sites were peritoneum ($n = 1$), adrenal gland ($n = 1$), liver ($n = 3$), and tumor thrombus ($n = 1$).

About 20% of the *BRAF*^{V600E}-mutated DTC patients showed ^{18}F-FDG uptake in the thyroid bed versus 4% in the *BRAF*^{V600E}-negative group. On the other hand, 26% of the *BRAF*^{V600E}-negative DTC patients showed ^{18}F-FDG–avid metastases uptake in the skeleton versus 6% in the *BRAF*^{V600E}-positive group (Table 2). There was a statistically significant difference regarding the sites' thyroid bed ($P = 0.008$), lymph node ($P = 0.031$), and bone ($P = 0.049$, all Fisher exact test) between the *BRAF*^{V600E} and *BRAF*-WT groups.

DISCUSSION

The results of this study indicate that in DTC, ^{18}F-FDG uptake is significantly higher for tumors with *BRAF*^{V600E} mutations than for tumors that are *BRAF*-WT. In contrast, *BRAF*^{V600E} mutational status demonstrated no correlation with tumor ^{18}F-FDG uptake in PDTC, suggesting that in this disease, glucose metabolic activity is predominantly regulated by other signaling pathways. In our cohort, the tumors were not systematically tested for mutations other than *BRAF*^{V600E}, and tumors in the *BRAF*-WT group might harbor additional genetic defects that affect glucose metabolism.

High glucose metabolic rates of cancer cells are often explained as a consequence of proliferation: accelerated transcription and translation in proliferating cells decreases the adenosine triphosphate–to–adenosine diphosphate ratio, which causes allosteric effects on rate-limiting metabolic enzymes, thereby increasing glucose uptake. Although this explanation is widely accepted, it is at odds with the frequent clinical observation that some slowly proliferating malignancies (e.g., low-grade lymphomas) or even premalignant lesions (e.g., colonic polyps) can be highly hypermetabolic on ^{18}F-FDG PET/CT studies (*14–16*).

An alternative, more recently proposed model is that activated oncogenes and inactivated tumor suppressors directly reprogram cellular metabolism. In this model, accelerated metabolic fluxes occur as a primary response to oncogenic signaling (*15*). This new model of tumor glucose metabolism implies that high ^{18}F-FDG uptake in cancer cells is not necessarily the consequence of rapid proliferation but is caused by the activation of oncogenic pathways that regulate transporters and enzymes involved in the metabolism of glucose.

Although there are ample preclinical data on the relationship between oncogene activation and glucose metabolism, clinical data are relatively scarce. One approach to gain some insight into the relationship between oncogene activation and glucose metabolism

TABLE 3
Lesion Analysis of ^{18}F-FDG–Positive *BRAF*^{V600E} and *BRAF*-WT Groups

Parameter	Value	DTC		PDTC	
		BRAF^{V600E}	*BRAF*-WT	*BRAF*^{V600E}	*BRAF*-WT
SUV_{max}	Median	6.3	4.7	6.4	9.4
	Minimum	1.6	1.1	1.9	2.3
	Maximum	51.2	30.1	30.0	47.0
CT size (cm)	Mean ± SD	1.6 ± 0.7	2.0 ± 1.5	1.9 ± 1.3	2.8 ± 1.9
	Median	1.3	1.7	1.5	2.2
	Minimum	0.6	0.4	0.6	0.6
	Maximum	3.8	7.8	4.5	8.0

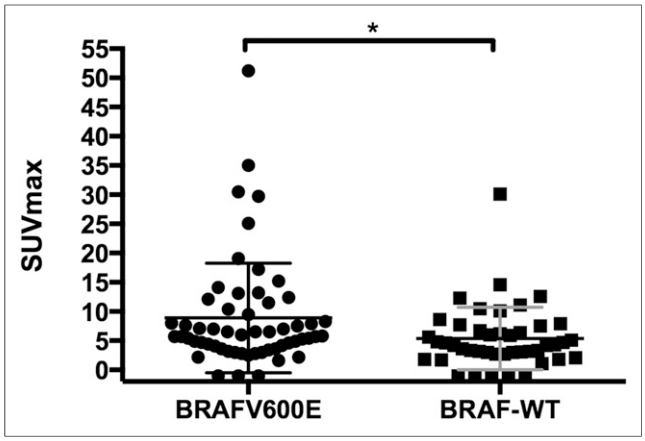

FIGURE 1. Comparison of SUV_{max} for DTC patients harboring *BRAF*^{V600E} mutation versus *BRAF*-WT. *P = 0.019.

in patients is to study the correlation between mutations in specific oncogenes and glucose metabolism. For instance, Parmenter et al. and Palaskas et al. showed a relationship between *BRAF* mutation and activation of mitogen-activated protein kinase downstream targets such as cMyc and Hif-1a and increased glucose metabolism for melanoma and basallike breast cancer, respectively (*12,17*).

Our findings are consistent with these observations, because *BRAF*^{V600E} DTCs demonstrated significantly higher ^{18}F-FDG uptake than *BRAF*-negative tumors.

In patients with multiple metastatic lesions, many approaches can be used to summarize overall metabolic activity. Measuring ^{18}F-FDG uptake of all lesions in a patient can be impractical, because thyroid cancer patients may demonstrate innumerable lung metastases that are difficult to separate on PET images. More importantly, patients with multiple metastases will skew the measured average ^{18}F-FDG uptake. Therefore, we limited our analysis to a maximum of 1 lesion in each of the 7 prespecified body regions. We also analyzed the single lesion with the highest ^{18}F-FDG uptake. Using both types of analyses, we found a significantly higher ^{18}F-FDG glucose metabolic activity for DTC with a *BRAF*^{V600E} mutation, suggesting that the observed differences are unlikely due to lesion selection. Patients with *BRAF*^{V600E} had significantly lower thyroglobulin values than patients with *BRAF*-WT

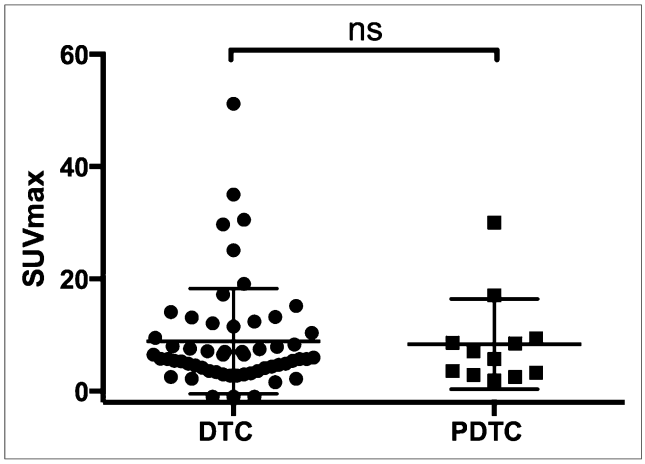

FIGURE 2. Comparison of SUV_{max} for DTC and PDTC patients harboring *BRAF* mutation. ns = nonsignificant. P = 0.91.

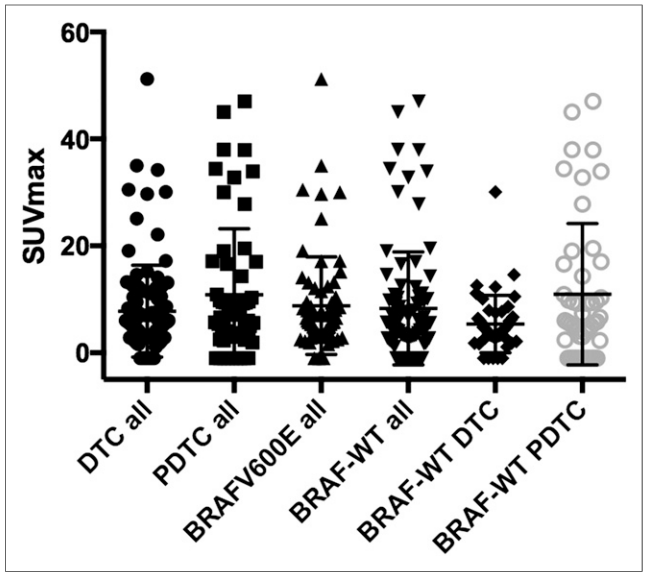

FIGURE 3. Distribution of SUV_{max} for all DTC and PDTC lesions, all *BRAF*-positive vs. -negative lesions, and *BRAF*-WT DTC vs. *BRAF*-WT PDTC lesions. There is a difference in SUV_{max} distribution of *BRAF*-WT DTC and *BRAF*-WT PDTC, even though results are not significant.

tumors. Thus, the higher ^{18}F-FDG uptake of *BRAF*^{V600E} tumors on PET cannot be explained by a higher tumor load.

There was no difference between the SUV_{max} of *BRAF*^{V600E}-positive DTC and *BRAF*^{V600E}-positive PTDC. The number of *BRAF*^{V600E}-positive PDTC patients was quite small, limiting the strength of the statistical analysis. Interestingly, ^{18}F-FDG uptake was approximately twice as high for *BRAF*-WT PDTC than for *BRAF*-WT DTC (Fig. 3). Consequently, we did not observe higher SUV_{max} for the overall group of *BRAF*-WT PDTC than *BRAF*-WT DTC.

In addition to differences in the metabolic activity of *BRAF*^{V600E} DTC and *BRAF*-WT DTC, we also found differences in their metastatic spread. *BRAF*^{V600E}-positive DTC tumors recurred more frequently to the lymph nodes and thyroid bed, whereas the *BRAF*-WT more often metastasized to bones, even though the number of follicular variants of the PTCs was low in both groups. This information might be helpful for the clinician when selecting specific imaging modalities for the workup of patients with rising thyroglobulin levels. In contrast, the SUV differences between *BRAF*^{V600E} and *BRAF*-WT in DTC and PDTC were too small to limit ^{18}F-FDG PET/CT imaging to *BRAF*^{V600E}-positive tumors. Therefore, our data do not support restricting ^{18}F-FDG PET/CT imaging to patients with PDTC.

The following limitations of our study should be noted. First, images were acquired by several PET scanners that differed in their sensitivity and spatial resolution. This difference may have contributed to the overlap of SUVs for the studied patient groups. Moreover, 53% of the lesions were smaller than 1.3 cm in diameter, and therefore partial-volume effects heavily influenced their SUVs. We could exclude a systematic difference of lesion size between the studied patient groups; nevertheless, partial-volume effects have likely contributed to the random variability of the SUV measurements.

Second, *BRAF*^{V600E} status and tumor differentiation were assessed for the resected primary tumor at the time of initial diagnosis. However, in many patients, ^{18}F-FDG PET/CT was performed several years later—accordingly, some of the tumors classified as DTCs at initial diagnosis may have evolved into PDTC. This time difference between

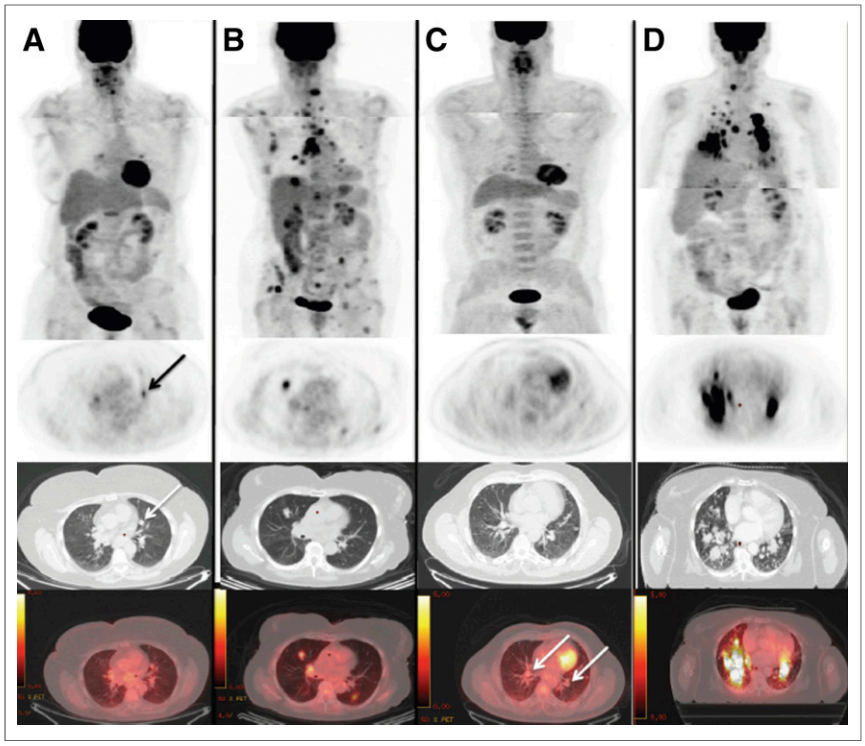

FIGURE 4. ^{18}F-FDG PET/CT scans in metastatic thyroid cancer patients with and without *BRAF*^{V600E} mutations. All PET images are scaled from 0.0 to 5.0 g/mL to allow for visual comparison of ^{18}F-FDG uptake. PET scans were acquired in 2 steps (patients' arms raised for images of chest and arms down for images of neck) to improve image quality. (A) A 66-y-old woman harboring DTC *BRAF*-WT showing lung nodule (1.1 cm in diameter on CT) with low ^{18}F-FDG uptake (arrows). (B) An 83-y-old woman harboring DTC *BRAF*^{V600E} with multiple ^{18}F-FDG–positive lesions with high uptake. (C) A 64-y-old man harboring PDTC BRAF-WT with multiple lung nodules (up to 1.5 cm in diameter on CT; arrows) with low/no ^{18}F-FDG uptake. (D) A 75-y-old woman harboring PDTC *BRAF*^{V600E} with multiple lung nodules showing high 18F-FDG uptake.

diagnosis and PET/CT imaging may also explain some of the overlap between the analyzed patient groups, as well as the high number of bone lesions. We must also acknowledge that tumor differentiation and *BRAF* status may be different between the primary tumor and metastases, because only primary thyroid tumors were analyzed for mutational status and we were unable to provide histopathologic data of the metastasis. However, it is more likely that the same mutational status of the primary tumor is found in the distant metastases (*18*).

Additionally, a selection bias may occur, because in a clinical setting not all patients will undergo an ^{18}F-FDG PET scan—only those who have a high-risk tumor, who exhibit clinical signs of progressive disease, or when the tumors have lost the ability to accumulate radioiodine. In our study, all of the patients were radioiodine-negative and had evidence of tumor progression state (increasing thyroglobulin values or progressive lesions in CT). Therefore, it is unlikely that the observed differences in ^{18}F-FDG uptake between *BRAF*-WT and *BRAF*^{V600E} tumors are related to different indications for performing the PET/CT scan. Nevertheless, we cannot rule out the possibility that some of the ^{18}F-FDG–negative lesions seen on CT represented treated disease, which may have increased the scatter of the SUV measurement in all patient groups.

CONCLUSION

In this retrospective study, *BRAF*^{V600E} DTC patients show a significantly higher ^{18}F-FDG uptake than *BRAF*-WT. Moreover, *BRAF*^{V600E} DTC patients show a higher number of ^{18}F-FDG–positive tumor manifestations in the thyroid bed, whereas the *BRAF*-WT patients show a higher number of bone metastases. The *BRAF*^{V600E} mutation had no significant effect on ^{18}F-FDG uptake in PDTC in our retrospective study, but the patient population is too small to draw definitive conclusions for this subtype of thyroid cancer.

REFERENCES

1. Kim BS, Ryu HS, Kang KH. The value of preoperative PET-CT in papillary thyroid cancer. *J Int Med Res.* 2013;41:445–456.
2. Kim M-H, Ko SH, Bae J-S, et al. Non–FDG-avid primary papillary thyroid carcinoma may not differ from FDG-avid papillary thyroid carcinoma. *Thyroid.* 2013;23:1452–1460.
3. Kim BH, Kim S-J, Kim H, et al. Diagnostic value of metabolic tumor volume assessed by ^{18}F-FDG PET/CT added to SUVmax for characterization of thyroid ^{18}F-FDG incidentaloma. *Nucl Med Commun.* 2013;9:868–876.
4. Robbins RJ, Wan Q, Grewal RK, et al. Real-time prognosis for metastatic thyroid carcinoma based on 2-[^{18}F]fluoro-2-deoxy-D-glucose-positron emission tomography scanning. *J Clin Endocrinol Metab.* 2006;91:498–505.
5. Bertagna F, Treglia G, Piccardo A, Giubbini R. Diagnostic and clinical significance of F-18-FDG-PET/CT thyroid incidentalomas. *J Clin Endocrinol Metab.* 2012;97:3866–3875.
6. Caronia LM, Phay JE, Shah MH. Role of BRAF in thyroid oncogenesis. *Clin Cancer Res.* 2011;17:7511–7517.
7. Kimura ET, Nikiforova MN, Zhu Z, Knauf JA, Nikiforov YE, Fagin JA. High prevalence of BRAF mutations in thyroid cancer: genetic evidence for constitutive activation of the RET/PTC-RAS-BRAF signaling pathway in papillary thyroid carcinoma. *Cancer Res.* 2003;63:1454–1457.
8. Grabellus F, Nagarajah J, Bockisch A, Schmid KW, Sheu S-Y. Glucose transporter 1 expression, tumor proliferation, and iodine/glucose uptake in thyroid cancer with emphasis on poorly differentiated thyroid carcinoma. *Clin Nucl Med.* 2012;37:121–127.
9. Soares P, Lima J, Preto A, et al. Genetic alterations in poorly differentiated and undifferentiated thyroid carcinomas. *Curr Genomics.* 2011;12:609–617.
10. Grabellus F, Worm K, Schmid KW, Sheu S-Y. The BRAFV600E mutation in papillary thyroid carcinoma is associated with glucose transporter 1 overexpression. *Thyroid.* 2012;22:377–382.
11. Xing M, Alzahrani AS, Carson KA, et al. Association between BRAF V600E mutation and mortality in patients with papillary thyroid cancer. *JAMA.* 2013;309:1493–1501.
12. Parmenter TJ, Kleinschmidt M, Kinross KM, et al. Response of BRAF-mutant melanoma to BRAF inhibition is mediated by a network of transcriptional regulators of glycolysis. *Cancer Discov.* 2014;4:423–433.
13. Yun J, Rago C, Cheong I, et al. Glucose deprivation contributes to the development of *KRAS* pathway mutations in tumor cells. *Science.* 2009;325:1555–1559.
14. Schöder H, Noy A, Gönen M, et al. Intensity of ^{18}fluorodeoxyglucose uptake in positron emission tomography distinguishes between indolent and aggressive non-Hodgkin's lymphoma. *J Clin Oncol.* 2005;23:4643–4651.
15. Ward PS, Thompson CB. Metabolic reprogramming: a cancer hallmark even Warburg did not anticipate. *Cancer Cell.* 2012;21:297–308.
16. Israel O, Yefremov N, Bar-Shalom R, et al. PET/CT detection of unexpected gastrointestinal foci of ^{18}F-FDG uptake: incidence, localization patterns, and clinical significance. *J Nucl Med.* 2005;46:758–762.
17. Palaskas N, Larson SM, Schultz N, et al. ^{18}F-fluorodeoxy-glucose positron emission tomography marks MYC-overexpressing human basal-like breast cancers. *Cancer Res.* 2011;71:5164–5174.
18. Ricarte-Filho JC, Ryder M, Chitale DA, et al. Mutational profile of advanced primary and metastatic radioactive iodine-refractory thyroid cancers reveals distinct pathogenetic roles for BRAF, PIK3CA, and AKT1. *Cancer Res.* 2009;69:4885–4893.